Volume 35, Number 1

July 2004
ISSN 8756-3282

# BONE

Official Journal of the International Bone and Mineral Society

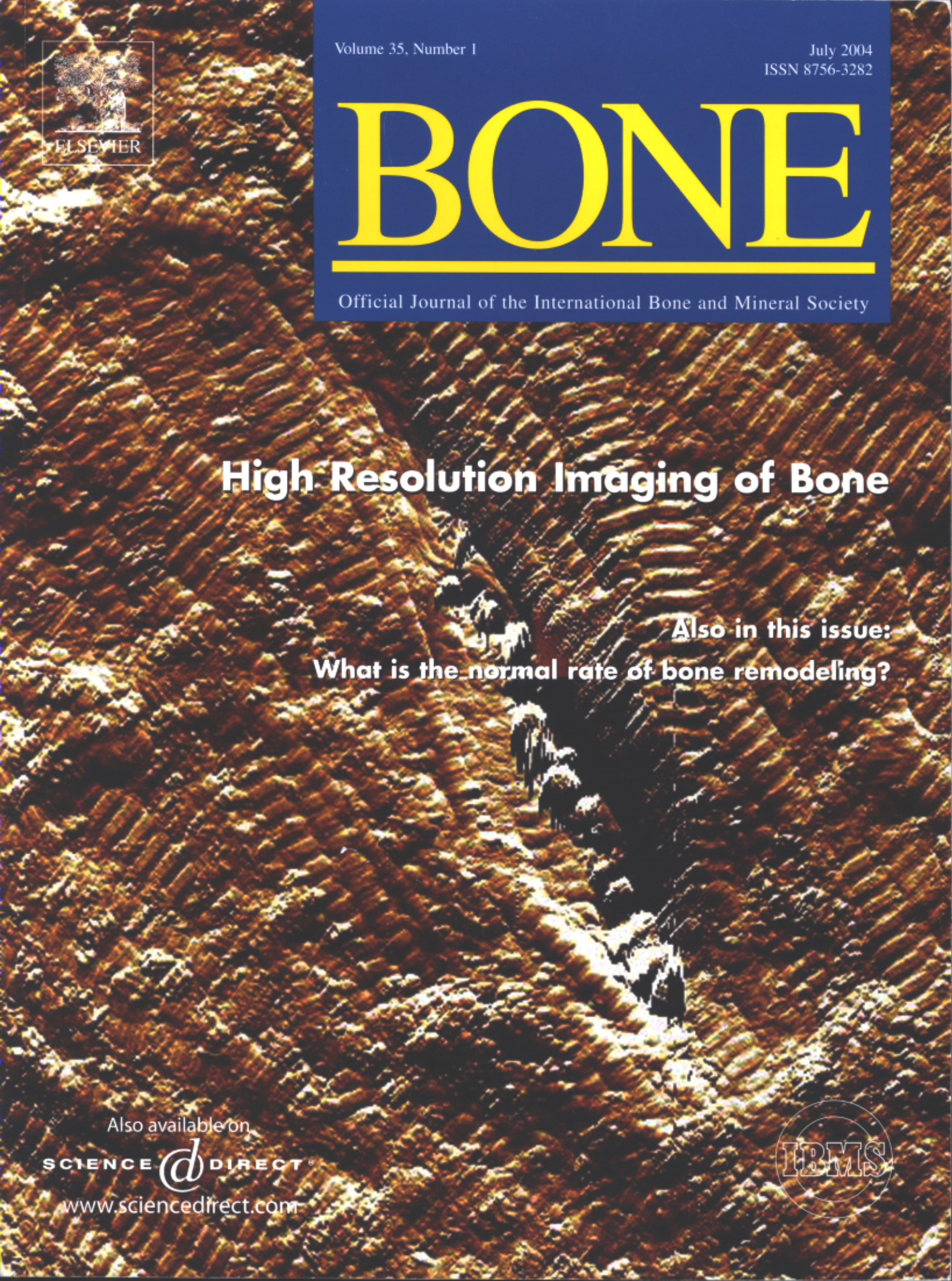

## High Resolution Imaging of Bone

Also in this issue:
What is the normal rate of bone remodeling?

ELSEVIER

Bone 35 (2004) 4–10

BONE

www.elsevier.com/locate/bone

# High-resolution AFM imaging of intact and fractured trabecular bone

Tue Hassenkam,[a,*] Georg E. Fantner,[a] Jacqueline A. Cutroni,[a] James C. Weaver,[b] Daniel E. Morse,[b] and Paul K. Hansma[a]

[a] *Department of Physics, University of California, Santa Barbara, CA 93106, USA*
[b] *Institute for Collaborative Biotechnologies, University of California, Santa Barbara, CA 93106, USA*

Received 12 December 2003; revised 13 February 2004; accepted 20 February 2004

**Abstract**

Nanoscale structural analyses of biomineralized materials can frequently help elucidate important structure–function relationships in these complex organic–inorganic composites. Atomic force microscope (AFM) imaging of the exterior surface of trabecular bone reveals a densely woven structure of collagen fibrils, banded with a 67-nm periodicity, and densely packed mineral plates. The mineral plates on the collagen fibrils overlap and exhibit a large range of plate diameters from 30 to 200 nm. On the collagen fibrils, small nodular features, spaced 20–30 nm, run perpendicular to the fibrils. In some cases, these nodules are also seen on filaments extending between collagen fibrils. We hypothesize that these protrusions are noncollagenous proteins such as proteoglycans and may have collapsed into compact structures when the sample was dried. AFM images of pristine fractured surfaces reveal a dense array of mineral plates. In a few isolated locations, short sections of bare collagen fibrils are visible. In other regions, the existence of the underlying collagen fibrils can be inferred from the linear patterns of the mineral plates. Fractured samples, rinsed to remove mineral plates, reveal separated collagen fibrils on the fractured surfaces. These fibrils are often covered with protrusions similar to those observed on the exterior surfaces but are less organized. In addition, as on the exterior surfaces, there are sometimes small filaments extending between neighboring collagen fibrils. These studies provide important insights into the nanostructured architecture of this complex biocomposite.


*Keywords:* Nanostructure; Trabecular bone; AFM, Atomic force microscope; Mineral plates; Collagen fibrils

## Introduction

Understanding the mechanics of living bone continues to be a major scientific challenge, as pointed out by Weiner et al. [1] and Zioupos et al. [2] in their impressive work and emphasized by others [3–6]. An important aspect of this challenge is understanding of the nanoscopic interplay between the basic building blocks of bone [7,8]. It is known that bone is primarily composed of mineralized collagen fibrils [9]. Imaging these mineralized fibrils and their structural relations inside bone is a daunting task since both the fibrils and the mineral plates are very small. There has been recent progress, however, with light [3,10], electron [3,11–13], and scanning probe microscopy, both on mineralized tendon [14,15] and bone [16,17]. Nevertheless, mapping the structural layout of mineralized collagen fibers, within their natural environment of healthy bone, remains a challenge. Here, we show atomic force microscope (AFM) images of the exterior and interior of fresh trabecula taken from a bovine vertebrae. These images reveal a woven layer of lightly mineralized fibrils on the surface of the trabecula and an interlocking network of more heavily mineralized fibrils in the trabecular interior.

## Materials and methods

Fresh bovine vertebrae were cut into 5 × 5 × 4 mm cubes with a conventional band saw and a diamond band saw. The cubes were cleaned with pressurized water to remove soft organic matter (i.e., bone marrow). Under an optical microscope, the cubes were studied to find single trabecula that was not touched by the saw blade during the cutting of the bone and that were accessible to the AFM. The sample cubes were then dried and glued to metal disks with Devcon 2-ton epoxy. Images were recorded in air, at room temperature, and at a scan rate of 1 Hz, using standard

* Corresponding author.
*E-mail address:* tue@nano.ku.dk (T. Hassenkam).

8756-3282/$ - see front matter © 2004 Elsevier Inc. All rights reserved.
doi:10.1016/j.bone.2004.02.024

tapping mode atomic force microscopy (Digital Instruments Nanoscope IV), equipped with silicon cantilevers (force constant 40 N/m, resonant frequency 300 kHz, nanodevices tap 300).

## Results

Figs. 1A–C show stitched AFM amplitude images of three different parts of a single dehydrated trabecula that had been rinsed with water. The trabecula was about 150 μm in diameter and 350 μm long. Collagen fibrils are the dominant feature in these images; this is evident from the clearly visible 67 nm banding pattern observed in all the fibrils [18]. The width of these fibrils ranges from 50 to 200 nm, with an average of approximately 100 nm. The thickness of individual fibrils could only be measured in a few cases, where it averaged about 20 nm, which suggests that the cross section of the fibrils is oval in shape. This may, however, be an artifact due to drying [19,20].

The length of the fibrils is difficult to estimate from these images due to the woven structure of the composite, but the fibrils are at least several micrometers long. In some cases, the fibrils seem to divide into two Y-shaped fibrils (blue arrowhead in Fig. 1A). In other cases, it seems that several fibrils interlock to form larger superstructures with shifts in the banding pattern from one fibril to the next, which is evident in Fig. 1B (blue arrowhead).

Fig. 1A shows the surface from the end of the trabecula, where the collagen fibrils do not seem to have a preferred orientation; a few bundles of five to six collagen fibrils share the same orientation. Fig. 1B displays a region from the middle part of the trabecula. Here, the surface is even more rugged, with individual fibrils arranged in a crisscross pattern, especially in the lower portion of the image. Fig. 1C shows a region from the other end of the trabecula. Here, most fibrils form huge bundles oriented in the same direction. However, there are large voids in the fibrillar fabric, which resemble those revealed by SEM (Fig. 1D). In all three AFM images, aggregates of nodules or protrusions are attached to the exterior of the collagen fibrils; these are most evident in Fig. 1C.

Higher resolution images of these protrusions are shown in Fig. 2. The underlying banding pattern of the collagen indicates the direction of the fibrils. Protrusions of about the equal size (10–30 nm in diameter) and morphology (oval shape) are attached to the collagen fibrils. While it is possible that these features could have different origins, some are probably mineral plates but may also be noncollagenous proteins. In some cases, aggregates of protrusions form orthogonal bridging between two adjacent collagen fibrils, as indicated by white arrows. In these bridges, as well as on the fibrils themselves, the protrusions sometimes form aggregates with separations of 15–30 nm. We believe that these bridges and some of the protrusions are noncollagenous protein assemblies.

Some areas on the surface of the trabeculae are almost completely covered with mineral plates (Fig. 3). The thickness of the plates varies from 3 to 10 nm, while the width and length typically range from 30 to 120 nm but can be up to 200 nm. Interestingly, the spacing between the centers of some of the plates is around 70 nm (an example is marked by a black arrow), which is close to the 67-nm banding seen in collagen. Bare collagen can be seen in several places in the image (the clearest examples are marked by white arrows), indicating the direction of the underlying collagen fibrils at these particular spots. Though there is no particular order to the mineral plates, there are small regions of local order, indicating a stacking direction of the mineral plates.

To investigate the trabecular interior, we began fracturing trabeculae with a razor blade. Care was taken not to actually cut the sample, but pull it apart to get pristine fractured surfaces. Fig. 4 shows AFM amplitude images from the fractured surfaces. The particles in these images resemble those seen in Fig. 3. Both have dimensions consistent with mineral plates (3–10 nm in thickness, 30–120 in diameter). No bare collagen fibrils are visible, but especially in Fig. 4B, the 67-nm banding of collagen appears repeated in the spacing of the mineral plates that appear to follow underlying collagen fibrils. The images shown in Fig. 4 are representative of about 30 images obtained from the fractured surface; none show networks of bare collagen fibrils.

Fig. 5 shows the same fractured surface after it was rinsed in water to partly demineralize it (demineralization makes it easier to see the 67-nm banding pattern on collagen fibrils). Besides the presence of more debris on the surface, the morphology of the sample is similar to the morphology of the outside of the trabeculae. The fibrils are also bridged by small threads, approximately 20 nm in diameter (white arrows and insets). In contrast to Fig. 1, where the collagen fibrils are closely packed, here in Fig. 5, the collagen fibrils have been torn apart.

Fig. 6 shows an SEM image of a trabecular bone microcrack. Here, disrupted fibrils project into the microcrack and lie loosely on the fractured surfaces. The inset shows an AFM image from Fig. 5, rescaled to match the size scale of the SEM image. The inset suggests that the fibrils seen in the SEM image are indeed individual collagen fibrils.

## Discussion

The woven collagen fibril orientations, seen in Figs. 1A and B, do not seem to match the simple plywood model with parallel fibrils spanning several micrometers, which is believed to be a general structural motif for bone [18]. It is possible, however, that the structure seen in the figures on the surface of the trabeculae is the periosteum, which may have a completely different structure than the interior.

The fibrillar structure from the middle part of the trabecula appears very rugged. It is possible that the inter-

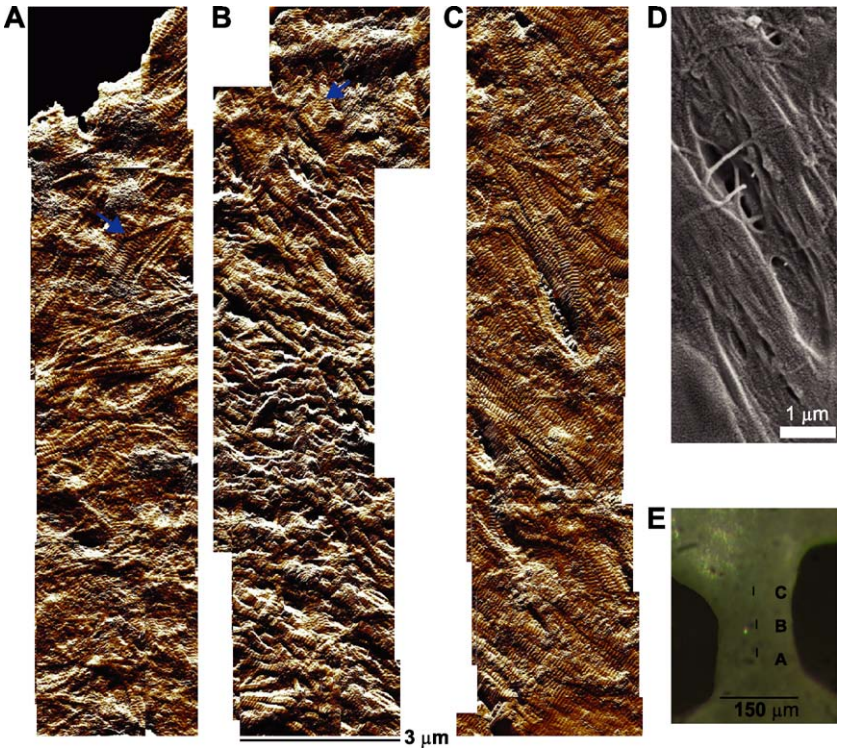


Fig. 1

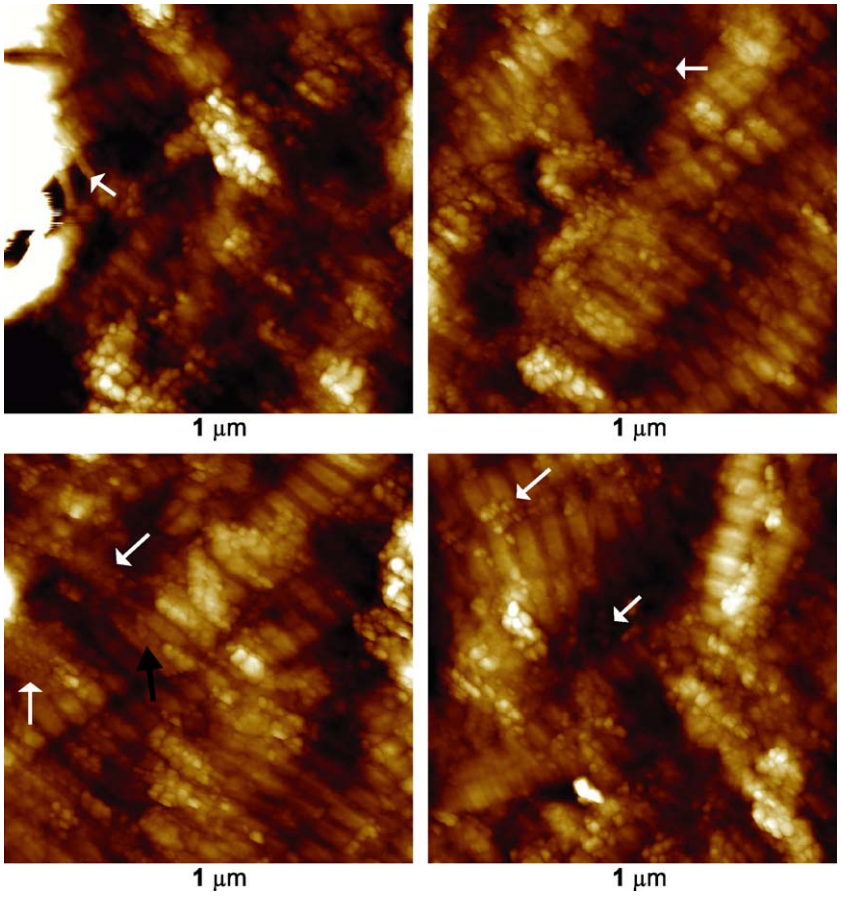


Fig. 2

locking fibrils evolved to give the center portion of the trabecula more strength because it would be a region of maximum stress during falls. It could also be that the trabecula in this region is damaged and that what is seen is the effect of internal microcracks propagating to the surface, which in turn could be the trabecula's way of signaling for remodeling, as originally proposed by Frost [21] an later put forward by Burr [22] in his review.

The ultrastructure of the surface seen in Fig. 2 reveals detailed information about the exterior of mineralized collagen fibrils. The fibrils' exterior is covered with aggregates of small protrusions, and in some places these aggregates form bridges between individual fibrils. The attachments of the aggregates on the collagen fibrils follow features in the fibrils' underlying structure. In almost every case, the aggregates follow a direction perpendicular to the direction of the collagen fibrils. This kind of bridging between collagen fibrils has been reported by Raspanti et al. [23] in the excellent work on rat corneal stroma and rat tail tendon [24], as proteoglycan bridging. We cannot distinguish if what we see in our images are proteoglycans, that there is a 15- to 30-nm repetition pattern consistent with the distance between core proteins on a hyaluronic polymer backbone [25], points in this direction.

We believe that the structures in Fig. 3, and to some extent on Fig. 4, result from mineral plates attached in an overlapping arrangement to the fibrils' exterior. This is supported by the spacing at several spots of about 67 nm, between the centers of neighboring mineral plates, indicating an intimate contact with the periodicity of an underlying collagen fibril. The literature recognizes that a substantial amount of mineral deposits in bone are in the intrafibrillar regions between and on the outside of collagen fibrils [18,26].

Direct viewing of dispersed crystals in the TEM has provided some of the best data to date on the ranges of their lengths and widths. Because of the need to disperse the crystals for TEM, breakage occurs and the estimated size ranges are biased towards the low range. Here this problem is avoided, and indeed the size range reported here (30–200 nm) is higher than those in the literature [12,27]. The range reported here may be as close to the in vivo range as has been achieved to date. It clearly shows that single crystals outgrow the gaps and cover large areas of fibrils. But our estimates of crystal thickness (3–10 nm) probably suffer from the same problem that plagued other attempts to use TEM images to measure thickness, it is very difficult to know that the crystal is really edge-on when making measurements. In this case, the SAXS measurements are probably more trustworthy. They report a thickness range from about 1.5 to 4 nm.

We have not seen any needle-shaped minerals in our study, which suggests that the vast majority of mineral plates are plate shaped. The larger mineral plates in Fig. 4 lie flat on the fibrils. This is consistent with previous work, including X-ray measurements [14,28,29], which showed that the mineral plates are oriented along fibrils with their *z*-axis perpendicular to the direction of the fibril. This fish-scale packing (which is our term for what has been previously observed by Weiner and Traub and confirmed by Landis: that almost all the crystals have their large surfaces aligned along the collagen fibrils) of the mineral plates on the collagen fibrils is common to the outside (Fig. 4) and the inside (Fig. 5) of the trabecula.

When a fractured surface is partly demineralized by rinsing the sample in water, the collagen fibrils become more apparent, as seen in Fig. 5. These fibrils are covered with small bumps similar to those on the collagen fibrils that are on the outside of the trabecula (Fig. 2). Small threads bridging between individual collagen fibrils are also seen on the fractured surfaces. The sizes of these threads are consistent with the sizes of the bridging threads found for the surface of the trabecula (Fig. 2). As can be seen in the SEM in Fig. 6, fibrils both span a microcrack and cover the fractured surfaces after partial demineralization. Some of these fibrils are probably individual collagen fibrils since the size scale of some fibrils match that of the fibrils in Fig. 4, where they are conclusively shown to be collagen fibrils because of the 67-nm banding. The fractured surfaces in both the AFM and the SEM images seem dominated by collagen fibrils. These collagen fibrils are clearly disturbed by the fracturing, while the mineral plates seem unaffected (Fig. 4). This clearly illustrates the importance of the organic matrix in the mechanics of bone [30].

It is clear from Figs. 5 and 6 that individual fibrils in the gap are sticking to other fibrils at several places, suggesting that attachments between neighboring fibrils play an important role in energy dissipation in the microcrack and consequently in the energy dissipation of the whole bone. The binding agent that makes these collagen fibrils adhere to one another could be the bridges seen in Figs. 2 and 5, in addition to the interlocking of the fibrils seen in Fig. 1.

In summary, we find that a dense network of interconnected collagen fibrils covers the outside of the

Fig. 1. The figure shows three 3 × 13.6 μm stitched AFM amplitude images (A, B, and C) of the surface of a trabecula at three different locations, probably the periosteum. This surface had been rinsed with water, which may have removed mineral plates to reveal the fibrils of the organic matrix. The locations of the images relative to each other on the trabecula are indicated, to scale, on an optical image of the trabecula (E). Also shown in the figure is an 8 × 3.2 μm SEM image (D) of a surface on a similar trabecula. All four insets show a woven fibril structure, it is clear from the 67-nm banding pattern in all three AFM images that the fibrils are mostly made of collagen. The blue arrowheads indicate the locations of structural patterns that may contribute to interlocking between the collagen fibrils (see the text for details).

Fig. 2. The 1 × 1 μm AFM topography images of the surface of the same trabecula as in Fig. 1. We see aggregates bridging the fibrils in several places as indicated by white arrows. There are projections along these aggregates spaced by 20–30 nm.

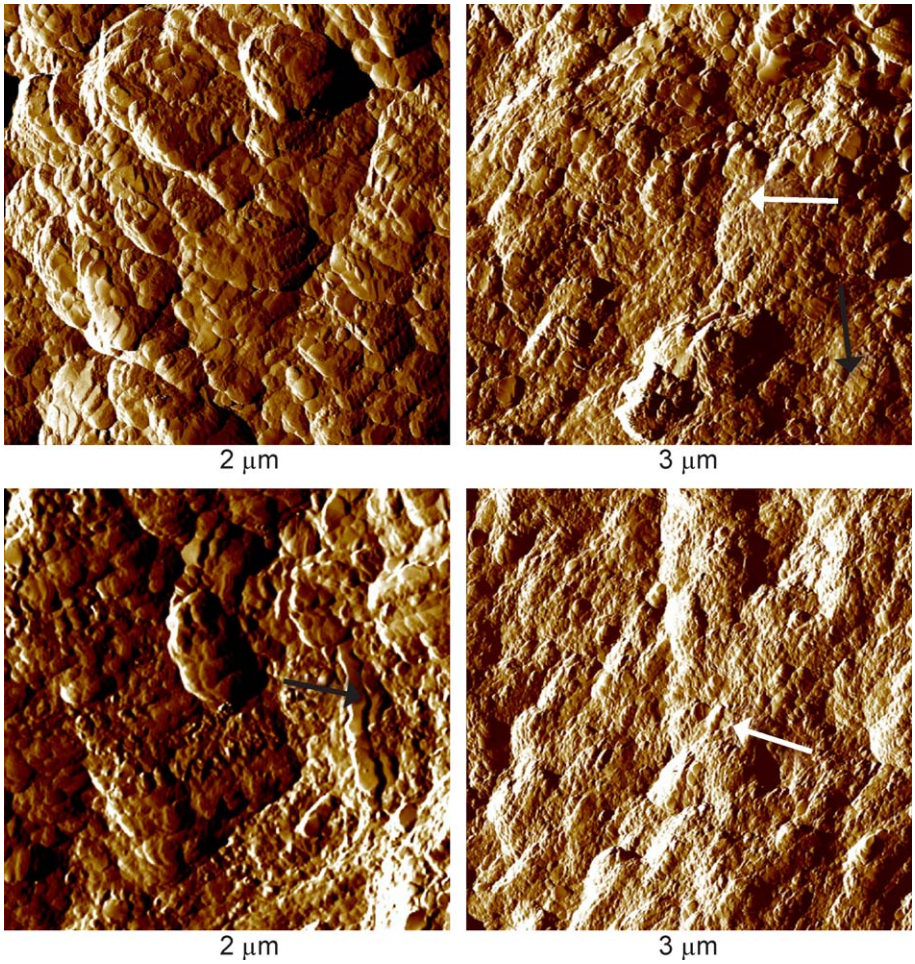


Fig. 3. The 3 × 3 μm AFM amplitude images of the surface of a trabecula with mineral plates still in place. A 67-nm spacing between individual plates is indicated by black arrowheads, suggesting a fish scale packing motif for the mineral plates on the collagen fibrils. Naked collagen fibrils are visible at white arrowheads.

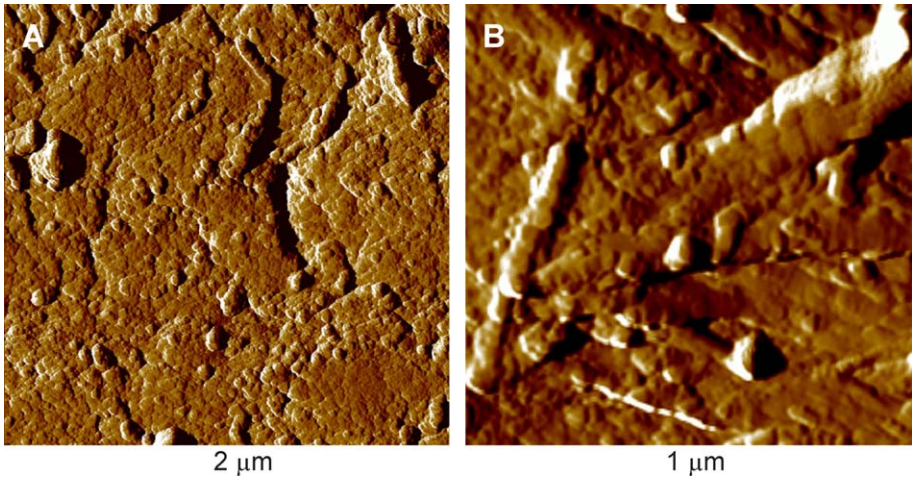


Fig. 4. (A) The 2 × 2 μm AFM amplitude images of the cleaved surface of a trabecula. The image is dominated by mineral plates. (B) The 1 × 1 μm AFM amplitude images of the cleaved surface of the trabecula on a different location. Here the image is also dominated by mineral plates, but a fibrillar structure showing mineral plates that pack like fish scales on the fibrils is also evident.

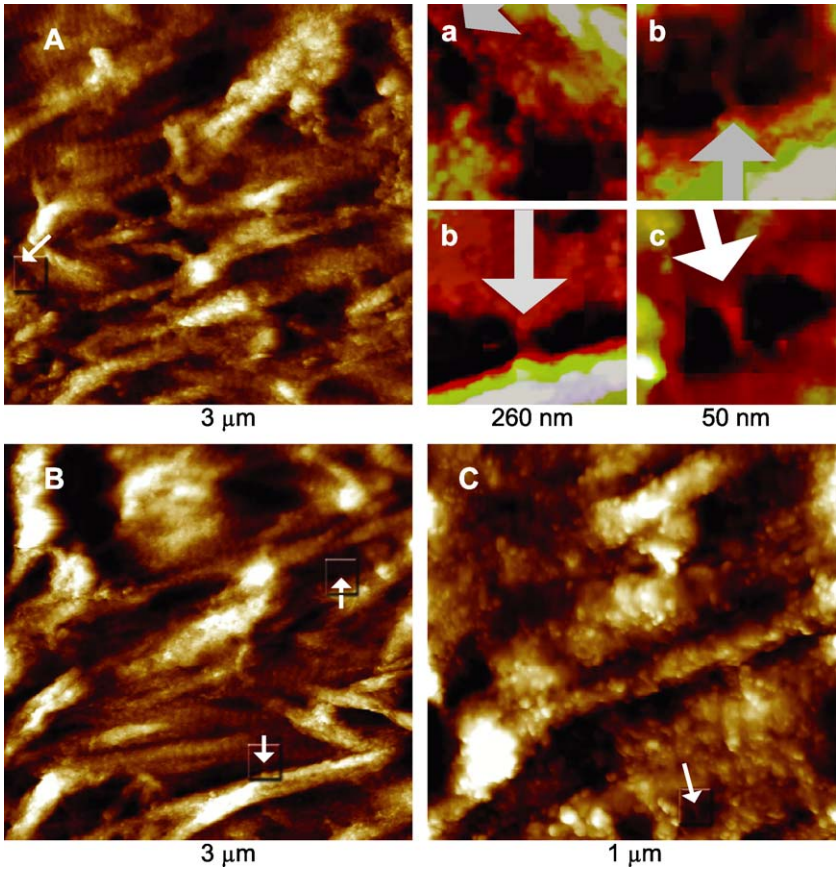


Fig. 5. (A, B, and C) AFM topography images from different regions of the fractured surface of a trabecula that has been partly demineralized by rinsing in water. Here the 67-nm banding pattern in the collagen is evident in all the fibrils. The small protrusions covering the collagen fibrils are probably noncollagenous proteins attached to the fibrils though there may be some remaining mineral plates as well. In some cases, bridging aggregates between individual collagen fibrils is clearly visible, see arrows in the full frame images and in the magnified and computer-enhanced small images (a is from A, b is from B, and c is from C).

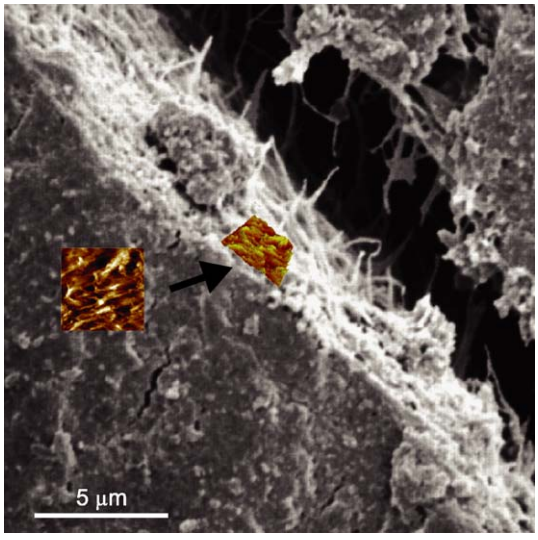


Fig. 6. SEM image of a trabecular bone microcrack. The insets show the AFM image from (Fig. 5B) scaled to fit the dimensions of the SEM image. A 3-D version of the AFM image is shown as an inset to ease the comparison, but it has no direct relation to the location shown in the SEM. Comparing the inset with the SEM image suggests that the fibrils seen spanning the gap in the SEM image are collagen fibrils.

trabecula after rinsing with water. There are interlocking polymers between and on the fibrils with a spacing of 15–30 nm. In addition, we see mineral plates attach to the outside of the collagen fibrils like scales on a fish. Fractured surfaces display mineral plates arranged in a similar manner to those on the surface of the trabecula. Partially demineralized fractured surfaces show disrupted collagen fibrils consistent with those seen in SEM images of microcracks.

## Acknowledgments

The research was supported by NASA/URETI on Bio Inspired Materials under award NCC-1-02037, NIH under award GM65354, NSF under award DMR-9988640, a research agreement with Veeco, and the UCSB Materials Research Laboratory under an NSF award DMR00-80034, the Institute for Collaborative Biotechnologies through grant DAAD19-03-D-0004 from the U.S. Army Research Office, and the NOAA National Sea Grant College Program, U.S. Department of Commerce (NA36RG0537,

Project R/MP-92) through the California Sea Grant College System, and the Danish research councils (STVF).

## References

[1] Weiner S, Traub W, Wagner HD. Lamellar bone: structure–function relations. J Struct Biol 1999;126:241–55.
[2] Zioupos P, Currey JD, Casinos A. Tensile fatigue in bone: are cycles-, or time to failure, or both, important? J Theor Biol 2001; 210:389–99.
[3] Lui D, Wagner HD, Weiner S. Bending and fracture of compact circumferential and osteonal lamellar bone of the Baboon tibia. J Mater Sci, Mater Med 2000;11:49–60.
[4] Reilly GC, Curry JD. The effects of damage and microcracking on the impact strength of bone. J Biomech 2000;33:337–43.
[5] Rho JY, Kuhn-Spearing L, Zioupos P. Mechanical properties and the hierarchical structure of bone. Med Eng Phys 1998;20:92–102.
[6] Heaney RP. Is the paradigm shifting? Bone 2003;33:457–65.
[7] Gao HJ, Ji BH, Jager IL, Arzt E, Fratzl P. Materials become insensitive to flaws at nanoscale: lessons from nature. PNAS 2003; 100:5597–600.
[8] Roschger P, Gupta HS, Berzanovich A, Ittner G, Dempster DW, Fratzl P, et al. Constant mineralization density distribution in cancellous human bone. Bone 2003;32:316–23.
[9] Weiner S, Lowenstam HA. On Biomineralization. Oxford: Oxford Univ. Press; 1989.
[10] Cadet ER, Gafni RI, McCarthy EF, McCray DR, Bacher JD, Barnes KM, et al. Mechanisms responsible for longitudinal growth of the cortex: coalescence of trabecular bone into cortical bone. J Bone Jt Surg, Am Vol 2003;85A:1739–48.
[11] Porter AE, Hobbs LW, Rosen VB, Spector M. The ultrastructure of the plasma-sprayed hydroxapatite-bone interface predisposing of bone bonding. Biomaterials 2002;23:725–33.
[12] Rosen VB, Hobbs LW, Spector M. The ultrastructure of anorganic bone and selected synthetic hydroxyapatites used as bone graft substitute materials. Biomaterials 2002;23:921–8.
[13] Rubin MA, Jasiuk L, Taylor J, Rubin J, Ganey T, Apkarian RP. TEM analysis of the nanostructure of normal and osteoporotic human trabecular bone. Bone 2003;33(3):270–82.
[14] Lees S, Prostak KS, Ingle VK, Kjoller K. The loci of mineral in Turkey leg tendon as seen by atomic-force microscope and electron-microscopy. Calcif Tissue Int 1994;55:180–9.
[15] Erts D, Gathercole LJ, Atkins EDT. Scanning probe microscopy of intrafibrillar crystallites in calcified collagen. J Mater Sci, Mater Med 1994;5:200–6.
[16] Baranauskas V, Garavello-Freitas I, Jingguo Z, Cruz-Hofling MA. Observation of the bone matrix structure of intact and regenerative zones of tibias by atomic force microscopy. J Vac Sci Technol A 2001;19:1042–5.
[17] Weismann HP, Chi LF, Stratmann U, Plate U, Fuchs H, Joos U, et al. Sutural mineralization of rat calvaria characterized by atomic-force microscopy and transmission electron microscopy. Cell Tissue Res 1998;294:93–7.
[18] Weiner S, Wagner HD. The material bone: structure–mechanical function relations. Annu Rev Mater Sci 1998;28:271–98.
[19] Gutsmann T, Fantner GE, Venturoni M, Ekani-Nkodo A, Thompson JB, Kindt JH, et al. Evidence that collagen fibrils in tendons are inhomogeneously structured in a tubelike manner. Biophys J 2003; 84:2593–8.
[20] Venturoni M, Gutsmann T, Fantner GE, Kindt JH, Hansma PK. Investigations into the polymorphism of rat tail tendon fibrils using atomic force microscopy. Biochem Biophys Res Commun 2003; 303:508–13.
[21] Frost HM. Bone microdamage: factors that impair its repair. In: Uhthoff HK, editor. Current Concepts in Bone Fragility. Berlin: Springer, 1985. p. 123–48.
[22] Burr DB. Targeted and nontargeted remodeling. Bone 2002;30:2–4.
[23] Raspanti M, Congiu T, Alessandrini A, Gobbi P, Ruggeri A. Different patterns of collagen-proteoglycan interaction: a scanning electron microscopy and atomic force microscopy study. Eur J Histochem 2000;44:335–43.
[24] Ottani V, Martini D, Franchi M, Ruggeri A, Raspanti M. Hierarchical structures in fibrillar collagens. Micron 2002;33:587–96.
[25] Ng L, Grodzinsky AJ, Patwari P, Sandy J, Plaas A, Ortiz C. Individual cartilage aggrecan macromolecules and their constituent glycosaminoglycans visualized via atomic force microscopy. J Struct Biol 2003;143:242–57.
[26] Katz EP, Li S. Structure and function of collagen fibrils. J Mol Biol 1973;80:1–15.
[27] Tong W, Glimcher MJ, Katz JL, Kuhn L, Eppell SJ. Size and shape of mineralites in young bovine bone measured by atomic force microscopy. Calcif Tissue Int 2003;75:592–8.
[28] Lees S. Mineralization of type I collagen. Biophys J 2003;85:204–7.
[29] Jaschouz D, Paris O, Roschger P, Hwang HS, Fratzl P. Pole figure analysis of mineral nanoparticle orientation in individual trabecular of human vertebral bone. J Appl Crystallogr 2003;36:494–8.
[30] Landis WJ. The strength of a calcified tissue depends in part on the molecular-structure and organization of its constituent mineral crystals in their organic matrix. Bone 1995;16:533–44.